Deterioration Assessment of Infrastructure Using Fuzzy Logic and Image Processing Algorithm

Haran Pragalath[1]; Sankarasrinivasan Seshathiri[2]; Harsh Rathod[3]; Balasubramanian Esakki[4]; and Rishi Gupta[5]

Abstract: The safety and serviceability of civil infrastructures have to be ensured either as part of a periodic inspection program or immediately following a given hazardous event. The use of digital imaging techniques to identify the deformed or deteriorated surfaces of structures is a substantial area of research and aims to investigate a number of unknown parameters, including damage quantification and condition rating. This manuscript illustrates the integration of previously developed fuzzy logic–based decision-making tools with the currently developed image processing algorithm to quantify the damage for the condition rating of civil infrastructures. The proposed integrated framework exploits visual specifics of different elements of the infrastructure to perform automated evaluation of structural anomalies such as cracks and surface degradation. Two different image segmentation tools, (1) bottom hat transform and (2) hue, saturation, color (HSV) thresholding, are applied to identify the surface defects. The developed image processing software is used with the fuzzy set framework proposed in the previous research to gauge the damage indices due to various deterioration types like corrosion, alkali aggregate reaction, freeze–thaw attack, sulfate attack, acid attack or loading, fatigue, shrinkage, and honeycombing. Case studies of a long-span bridge and a warehouse building are illustrated for concept validation. The refined comprehensive method is presented as a graphical user interface (GUI) to facilitate the real-time condition assessment of civil infrastructures. **DOI: 10.1061/(ASCE)CF.1943-5509.0001151.**

Author keywords: Image algorithms; Fuzzy set framework; Deterioration; Structural health monitoring; Graphical user interface (GUI); Structural condition damage index (SCI).

Introduction

Civil structural health monitoring (SHM) has become an important requisite for diagnosis of material conditions and structural integrity as a whole to ensure the safety of critical civil infrastructures (Chang et al. 2003). It involves the condition assessment of civil infrastructures such as bridges, heritage structures, dams, power plants, pipelines, and other offshore structures. SHM is an efficient tool that can provide early warnings not only to safeguard the structures but also for the safety of end users. SHM can serve as an important tool to facilitate periodic infrastructure inspections. In many parts of the world, civil infrastructure is under tremendous strain because of increased traffic loads; shortened construction time; and lack of resources for inspection, maintenance, and repair of structures. Moreover, inspection of civil infrastructures after natural calamities, hurricanes, tornados, and fire can also greatly benefit from innovative SHM techniques. The sudden collapse of structures, including bridges, can cause a high number of causalities. In these circumstances, SHM can be an invaluable tool to manage and maintain structural integrity and also guarantee the residual capacity of civil structures. Acquired knowledge on the condition of the structure through SHM paradigms will enable preventive measures to avoid catastrophic failures, leading to prolonged service life and ultimately reducing lifecycle cost. Structural evaluation in terms of strength, serviceability, and durability offers awareness to users and the public for maintenance, repair, rehabilitation, and decommissioning. The accumulated information can be maintained in a database that can help in formulating design guidelines for effective condition monitoring. One of the components of SHM is continuous monitoring using sensors and their related smart software (Dong et al. 2003). The present study describes the development of a graphical tool inculcating a fuzzy-system and image-processing module for appropriate estimation of the structural damage condition index (SCI). The collected information can be used as a database to formulate design guidelines for effective condition monitoring.

The initial sections of this paper describe the use of fuzzy logic developed by Jain and Bhattacharjee (2012a, b) for decision making and later to assess the damage indices for various structural defects such as corrosion, alkali aggregate reaction, sulfate attack, acid attack, fatigue, shrinkage, and honeycombing. A list of other deterioration mechanisms (along with their possible causes) not covered by this model can be found in the Portland Cement Association (PCA) guidelines (Portland Cement Association 2002). The more detailed findings presented in this paper are a result of integrating image algorithms with the fuzzy logic–based decision-making protocol that can be used to expedite the overall SHM process through automatic detection of multiple defects such as cracks, efflorescence, and other surface degradation, as shown in Fig. 1.

[1]Postdoctorate Researcher, Dept. of Civil Engineering, Vel Tech Univ., Chennai, Tamilnadu, India. E-mail: haran5441@gmail.com

[2]Research Associate, Centre for Autonomous System Research, Vel Tech Univ., Chennai, Tamilnadu, India. E-mail: sankarsrin@gmail.com

[3]Ph.D. Scholar, Dept. of Civil Engineering, Univ. of Victoria, Victoria, BC, Canada (corresponding author). ORCID: https://orcid.org/0000-0003-3306-7634. E-mail: hmrathod@uvic.ca

[4]Associate Professor, Centre for Autonomous System Research, Vel Tech Univ., Chennai, Tamilnadu, India. E-mail: esak.bala@gmail.com

[5]Associate Professor, Dept. of Civil Engineering, Univ. of Victoria, Victoria, BC, Canada. E-mail: guptar@uvic.ca

Note. This manuscript was submitted on April 16, 2017; approved on October 30, 2017No Epub Date. Discussion period open until 0, 0; separate discussions must be submitted for individual papers. This paper is part of the ***Journal of Performance of Constructed Facilities***, © ASCE, ISSN 0887-3828.

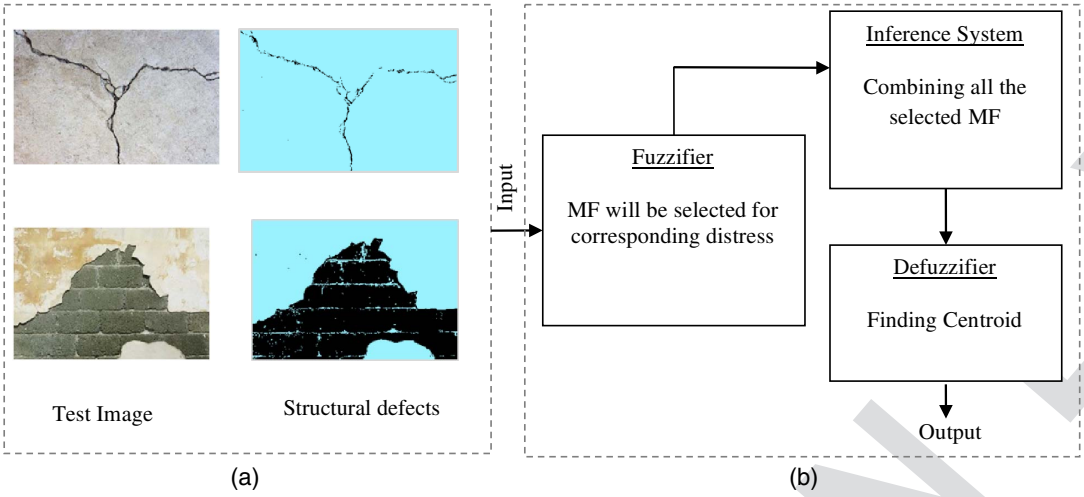

F1:1 **Fig. 1.** Integration of image processing tool with the fuzzy logic framework for decision making: (a) image analysis; (b) fuzzy concept

Recent trends in digital acquisition and image analysis are becoming a pivotal factor in nondestructive testing of civil structures (Yao and Pakzad 2012; Jahanshahi and Masri 2012). Novel digital protocols can bring radical advances over conventional strategies and expedite overall inspection activity significantly (Sankarasrinivasan et al. 2015; Jahanshahi et al. 2009). Such innovative protocols provide essential support for proficient monitoring and diagnosis activities. To establish such automated systems, the development of sophisticated image processing tools is the foremost requisite in assessing critical infrastructural defects. The authors believe that the developed software module can facilitate image-oriented or image-assisted evaluation and corresponding structural damage assessment with reduced uncertainty brought in by human judgment. The main objective of this manuscript is to demonstrate the development and application of this image-based software module for inspection of the civil infrastructure.

Fuzzy Approach for Condition Assessment of Structures

A fuzzy logic framework is an artificial intelligence technique to provide solutions to solve complex problems using linguistic terms (Mamdani and Assilian 1975). It involves the development of membership functions (MFs), fuzzy logic actions, and defuzzifications. MFs are used to characterize the fuzzy set based on whether the selected elements are discrete or continuous in representing a graphical form with an essence of fuzziness. MFs are classified into triangular, Gaussian, trapezoidal, and Z shaped. In general, triangular MFs are widely used because of their simplicity in constructing fuzzy sets (Zhao and Bose 2002). After selecting appropriate MFs, the relationship between input and output parameters is formulated by a set of linguistic statements called fuzzy rules, and normally IF–THEN rules are adopted. The number of fuzzy rules corresponds to the number of fuzzy sets for each input variable. The evaluation of conditional statements occurs in parallel to tune the system in a random manner. The assessed fuzzy rules are used to provide an output for any input within the range of the fuzzy processes. However, an output of fuzzy inference needs to be a scalar quantity to determine the performance characteristics of the considered system. For this, defuzzification is carried out to convert the fuzzy values into a required output in which a fuzzy quantity is transformed into a precise quantity.

Few researchers have used fuzzy set theory (FST) for the evaluation of deterioration of civil structures. Blockley (1975, 1977) used FST to deal with structures failing because of causes other than stochastic variations in loads and strengths. Brown and Yao (1983) and Wang and Elhag (2007) used FST as a decision-making tool for the damage assessment of a structure and subsequent repairs. Similarly, researchers have dealt with similar topics, such as structural damage assessment (Ogawa et al. 1984; Souflis and Grivas 1986; Savage et al. 1988; Hathout 1993; Furuta et al. 2000; Liang et al. 2001), performance evaluation (Hadipriono 1988), expert systems for damage assessment (Ross et al. 1990), and condition assessment ratings (Arliansyah et al. 2003; Sasmal et al. 2006; Sasmal and Ramanjaneyulu 2008). Fwa et al. (2003) proposed a condition rating and maintenance need assessment system for airport pavement using fuzzy logic systems, which related distress conditions directly to maintenance needs. Kim et al. (2006) reported a FST-based assessment system for reinforced concrete (RC) building structures to estimate the current state of buildings and to provide guidelines for future maintenance and management.

Visual inspection of any deteriorating structure is an integral aspect of routine assessment practices. Data collected through visual inspection are primarily qualitative and subjective because they rarely involve precise measurements and depend heavily on expertise of the site inspection team. To deal with these concerns, Jain and Bhattacharjee (2012a, b) have proposed a methodology using fuzzy concepts for visual inspection–based condition assessment. They developed a tool using the Visual Basic application that can be accessed in Microsoft *Excel*. The present study uses this framework of fuzzy logic (FL) to obtain the structural condition index of civil infrastructures, and its working principles are outlined further subsequently.

In the context of condition assessment, fuzzy logic formulation is carried out initially by selecting MFs and the parameters to define these MFs are based on the user inputs as per the condition rating of structural elements. These MFs are further processed to account for the severity of deterioration occurring either as local or global in a structural element by using linguistic hedges or modifiers. However, elements of any structure have many distresses; hence, each has to be assigned appropriate MFs. The accumulation of MFs is obtained using the fuzzy weighted average technique. These combined MFs are evaluated using a set of fuzzy rules, normally IF–THEN rules, which are used further for assessing the condition

of the structure. In the present study, various codes are assigned for different distresses and severity levels, and they have been used to determine the damage conditions of an element. The conclusions drawn from these fuzzy rules are made available as crisp output to the user in the defuzzification process using the centroid method.

To prepare these MFs, a series of questionnaires were prepared related to commonly occurring distress manifestations (such as corrosion, delamination, poor workmanship, and acid attack) and distributed among professionals (experts) from the field of construction engineering. This work was carried out by Jain and Bhattacharjee. This rating varies from 0 to 5, where "0" represents a condition that does not require any repair and "5" represents critical conditions that require immediate action (Jain and Bhattacharjee 2012a). This study reported questionnaire responses from 26 practicing senior experts or consultants, 3 scientists, 22 academicians, and 15 international experts. However, the responses from individual experts seemed to differ because of varied perceptions in predicting the distress rates of the structure. Hence, these observations need to be incorporated in a systematic way through developing membership functions in FST.

In the present study, various response data from individual experts are captured by following multiple steps to develop MFs. The collected response data are appropriately assigned a condition rating and evaluated further. Initially, if the intermediate condition rating is smaller than predecessor and successor, then the average of these ratings is considered an intermediate rating. For example, R_0, R_1, R_2, R_3, R_4, and R_5 are obtained as condition ratings, in which R_4 is lower than both R_3 and R_5, and R_4 is revised as the average of R_3 and R_5. In order to apply fuzzy set theory, the condition rating values should be in increasing order. Different condition ratings (R0 to R5) on the same structure are given based on the repair priority of the structure at once (no replicated inspections), as suggested in the literature by Mitra et al. (2010). In simple terms, experts could have different opinions on the same defects present in the structure or structural element. For example, a structure or structural element could be given any rating (R0 to R5) by an expert for the same deterioration mechanism or distress. Secondly, in order to neglect the small contribution of expert opinion in an evaluation of distress levels where the condition rating of the individual is less than the specific percentage of the summation of total respondents, then the same is updated to zero. A typical scenario where R_0 is less than a certain percentage (assume 10%) of summation of R_0, R_1, R_2, R_3, R_4, and R_5, means R_0 is updated to zero. Further, the condition ratings arrived at are normalized with respect to the peak number of responses. Later, the evaluated fractional values are considered as degrees of MFs (μ) corresponding to their condition ratings. The obtained MFs are modified using linguistic hedges and modifiers (Mitra et al. 2010) to account for local and global levels of defects, which are given by

$$\begin{aligned} Local:\ \mu_{x_i,local} &= \mu_{x_i}^{1/2} \quad \text{for } x_i \le x_0 \\ \mu_{x_i,local} &= \mu_{x_i}^{2} \quad \text{for } x_i \ge x_0 \end{aligned} \tag{1}$$

$$\begin{aligned} Global:\ \mu_{x_i,global} &= \mu_{x_i}^{2} \quad \text{for } x_i \le x_0 \\ \mu_{x_i,global} &= \mu_{x_i}^{1/2} \quad \text{for } x_i \ge x_0 \end{aligned} \tag{2}$$

where x_i = condition rating (0–5); and x_0 = condition rating where the MF is maximum.

The exponential term μ_x^2 involving the square of the MF values reduces the magnitude of the MF value at x. In contrast, $\mu_x^{1/2}$ increases the same. The use of modifiers ensures that if a certain severity of distress occurs "locally," then distress would warrant less repair action and "global" warrant higher repair action (Jain et al. 2012; Mitra et al. 2010).

The terms "local" and "global" are used in determining the extent of each distress and have been accounted by means of limits in the definition of membership functions. For example, the local extent will be considered if an element under study has ≤15% damage. Global will be considered if the damage is present all over the area under study. The philosophy behind this is given in the literature by Mitra et al. (2010).

So far, MFs have been developed for various defects individually. However, any structural element can undergo more than one deterioration, and that has to be accounted for in evaluating the damage condition of civil structures. In view of this, each distress can be assigned applicable MFs, and a generalized fuzzy rule will be formulated. In order to account for the combination of defects, a combined MF has to be developed using the following steps. MFs are initially rescaled using the following relation:

$$x_i^{j'} = \frac{x_i^j}{a - x_i^j} \tag{3}$$

where $x_i^{j'}$ = scaled condition rating for the ith MF at the jth distress; x_i^j = unscaled condition rating for the ith MF at the jth distress; and a = spread of the universe of discourse ≈5. To avoid any discontinuity, a has been assumed to be slightly greater than 5.0. (5.0001). As a user, you could select any value slightly greater (value + 1×10^{-3}) than the actual rating. If the actual rating value is used (in this case 5), then both a and x_i^j being 5 would render x_i^j mathematically undefined.

Further, by using the vertex method (Dong and Shah 1987), the scaled MFs are aggregated to obtain combined MFs as given by

$$\mu_i | x_i^{j'}$$

$$\text{for } \mu_i \in \{0, 0.1, 0.2, \ldots\ldots 0.9, 1.0, 1.0, 0.9, 0.8, \ldots\ldots, 0.2, 0.1, 0\} \tag{4}$$

where $x_i^{j'} = \sum_j x_i^{j'}$ = aggregation of MF on a modified scale.

Finally, the scaled MFs are reverted to the original scale using Eq. (5)

$$x_i^{j'} = \frac{a x_i^j}{1 + x_i^j} \tag{5}$$

where x_i = original scale rating corresponding to the MF value μ_i.

After formulating the combined distress effects, defuzzification is carried out using the centroid method (Madau and Feldkamp 1996). The centroid is calculated based on the following formula:

$$Centroid = \sum_{i=1}^{n} \frac{\frac{1}{6}(x_{i+1} - x_i)(2x_i y_i + x_{i+1} y_i + x_i y_{i+1} + 2x_{i+1} y_{i+1})}{0.5(x_{i+1} - x_i)(y_i + y_{i+1})} \tag{6}$$

where x = condition rating; y = degree of MFs; and i = number of areas, which varies from 1 to n.

The resulting centroid represents the condition index of an element. Initially, this is performed for all the elements that correspond to an individual deterioration mechanism. Later, using the weighted average method, structural condition indices will be determined. In the weighted average method, each element condition index is assigned with a weight depending upon the significance of

an element. The ratio of summation of the weighed condition index to the summation of weights is calculated as SCI to examine the damage condition of the structure.

In order to understand more clearly the distress manifestation conditions along with severity, a code is generated as deterioration–distress–severity–extent. For example, CORR-CRACK-MOD-G represents corrosion as deterioration, cracks as distress, severity at a moderate level, and extent as a global level, similar to previous work (Jain and Bhattacharjee 2012b). Similarly, MFs are generated for all the inspection condition codes. Different deterioration mechanisms considered in this study are corrosion, alkali aggregate reaction, freeze–thaw attack, sulfate attack, acid attack, fatigue, shrinkage, and honeycombing. The detailed procedure for developing MFs is explained further in the Appendix.

Image Algorithm for Detection and Quantification of Structural Defects

The formation of cracks is an early indication of deterioration, especially in reinforced concrete structures. Cracks can lead to reduction in the structural integrity of structures or catastrophic failure if not assessed properly and regularly. The traditional crack-monitoring methods are performed by professionals, and crack patterns have to be located and sketched manually. Such detection methods are laborious, time consuming, and subjective. In order to accelerate the process, an image processing–based crack detection method is suggested in this study and proven to be effective in estimating surface defects.

Jahanshahi et al. (2009) explored a survey of vision-based crack and corrosion detection approaches. Rose et al. (2014) reviewed experimental systems to determine the cracks in concrete bridges. Ikhlas et al. (2003) compared four crack detection techniques, namely the fast Haar wavelet transform (FHWT), fast Fourier transform (FFT), Sobel, and canny edge detectors. Yamaguchi et al. (2008) and Yamaguchi and Hashimoto (2010) considered a scalable image processing method to analyze larger images. Prasanna et al. (2012) proposed histogram-based feature extraction and a statistical interference algorithm to identify the cracks. Lattanzi and Miller (2014) exploited the intrinsic characteristics of images through segmentation based on the canny and K-means methods. Torok et al. (2014) reconstructed 3D profiles and subsequently measured the geometrical characteristics, including cracks, of collapsed building structures. Though crack detection algorithms are predominantly successful, the quantification aspect is still challenging and dependent on many practical issues (Zou et al. 2012). Limited research outcomes have been published, including morphological filters (Nguyen et al. 2012), scanning electron microscopy (Vidal et al. 2016), and depth-perception techniques (Jahanshahi and Masri 2013). In contrast to the prevailing literature, the proposed methodology uses a rapid and computationally inexpensive inspection system that can be operative for both color and grayscale images. This paper also highlights crucial parameters for structural damage forecasts, such as crack length and surface degradation.

In the subsequent section, an effective crack-detection algorithm is formulated considering both the morphological and color features of cracks. Hough-based filtration is adopted to eliminate unnecessary edges that do not represent cracks. In addition, a quantification of cracks is obtained based on the vision technique to examine the criticality of the damage to the infrastructure. A study has also been conducted to calibrate the developed model. The description of the proposed approach is given subsequently.

Morphological Approach

The morphological filter is widely used for the detection of structural patterns, feature analysis, and shape extraction from binary and grayscale images. Because concrete cracks possess some distinct patterns, this paper proposes a specific morphological filter for crack detection. In order to examine these characteristics, suitable image filters are to be incorporated. Initially, the test images are converted into grayscale, and the bottom hat transform is performed. Then, images are skeletonized and the Hough line filter is applied to remove the unnecessary regions. Finally, erosion and postprocessing of the filtered images provide the quantification of cracks. The detailed description of each morphological parameter is given subsequently.

Bottom Hat Transform (BHT)

BHT is a morphological filter capable of extracting image features that are dark toned and satisfy specific structural geometry. The mathematical expression is given by the difference of the image and its closing by a structural element, as in Eq. (6)

$$\mathrm{B\_out} = (\mathrm{Img\ s}) - \mathrm{Img} \tag{7}$$

where *Img* and s = the test image and structural element, respectively; and *B_out* is the output binary image. In a structure being studied by the authors, the structural element matrix of 3×3 size and the output correspond to pixel elements that are smaller in size. In general, the size of the structural element has to be calibrated on a par with acquisition parameters such as capturing distance and resolution. In order to evaluate the proposed image algorithms, various cracks on the walls are considered, which are shown in Fig. 2(a).

Though the performance of the BHT is satisfactory, the results obtained are often superfluous. They provide inaccurate information in real-time scenarios where thin dark edges resulting from wall curvature, door edges, and other corners of the structure appear as cracks. The simulation results for a random test image [Fig. 2(b)] using the BHT transform shows both cracks along with other erroneous dark edges or corners. Hence, it needs additional filtration to remove the excessive edges other than cracks.

Skeletonization

This process is carried out to convert the detected edges into a single pixel-wide line. During this process, redundant edge pixels are removed, which assists in the appropriate segmentation. Because the crack length quantization relies on a unique representation of cracks, this step is, foremost, important in removing surplus pixels. Once the skeletonizing is done, a Hough transform is applied to remove the edge segments that are perfectly straight.

Hough Line Elimination Filter

A Hough transform is a mapping of image pixels in the spatial (x, y) domain to (r, θ) Hough space. Under such a transformation, the presence of collinear points in the spatial domain is represented by a point with a similar angle and distance in Hough space. The problem of classifying dark corners and edges from the detected cracks is critical in crack quantification. Hence, this paper proposes the application of a Hough transform to identify straight line edges. Further, by setting a proper threshold, the unwanted edges can be nullified in the output image. Hence, the straight line edges present

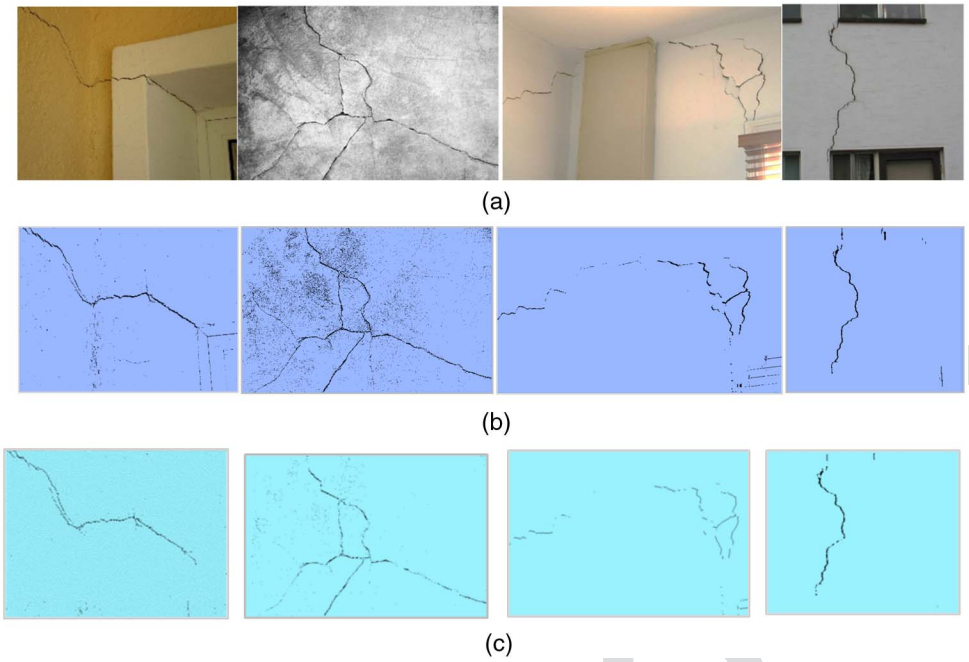

F2:1 **Fig. 2.** Test images and detection of cracks (a) various cracks on the walls; (b) BHT transform output; (c) improved crack results

in the output image can be eliminated by setting the proper threshold. Fig. 2(c) shows the output after incorporation of the Hough filter, where it can be clearly seen that all the straight line edges are removed except the cracks.

Erosion and Other Processing

Erosion removes all the insignificant regions that are negligible in relation to the detected segments. In particular, it is very effective in removal of isolated points and small regions that cannot be eliminated by Hough and BHT filters [Fig. 2(c)]. Further processing consists of removing isolated points and maintaining continuity of the edge pixels.

Hue, Saturation, Color (HSV) Thresholding—Color-Based Approach

In this approach, the color information of the test image is manipulated to discriminate crack pixels. The test images are converted from the red, green, blue (RGB) color space to the hue space for its robustness and accuracy. The HSV images are skeletonized, then a Hough line filter is applied to remove the unwanted regions. Further, erosion of images and postprocessing results in the quantification of cracks.

Extensive experiments have been conducted to derive the thresholding limit, and it has been found that cracks are characterized by lower saturation and value in HSV space. The algorithm was tested for various test images, and the results shown in Fig. 3 confirm the detection of cracks.

Quantification of Cracks

The data acquisition method and image protocols are of prime importance in quantifying cracks. The acquisition phase involves capturing images normal to the surface with an acquisition distance of 30–50 cm and an RGB image resolution of 640×480 pixels. A test database was created comprising 20 images with different crack lengths and widths. These images were taken during the evening hours in fairly bright conditions.

To validate the accuracy of the developed protocols, some of the sample database images are tested using the image segmentation approach to detect the edges of cracks and later used to find the crack width and length. In this approach, initially, the test images are converted into binary images. The cracks and void structures to be segmented should differ greatly in contrast from the background. The gradient and threshold of the test images have been calculated and applied to create a binary mask containing the segmented cracks and voids. In order to achieve these tasks, edge and Sobel operators have been used. Fig. 4(a) shows images of concrete prisms that have undergone flexural loading. There are black lines on the specimens that were drawn using black ink to facilitate positioning of the specimens during testing. These drawn lines do not

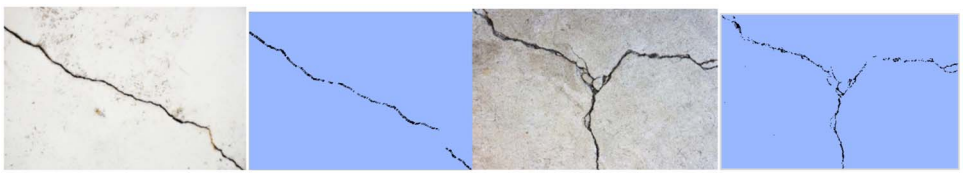

F3:1 **Fig. 3.** HSV thresholding crack output

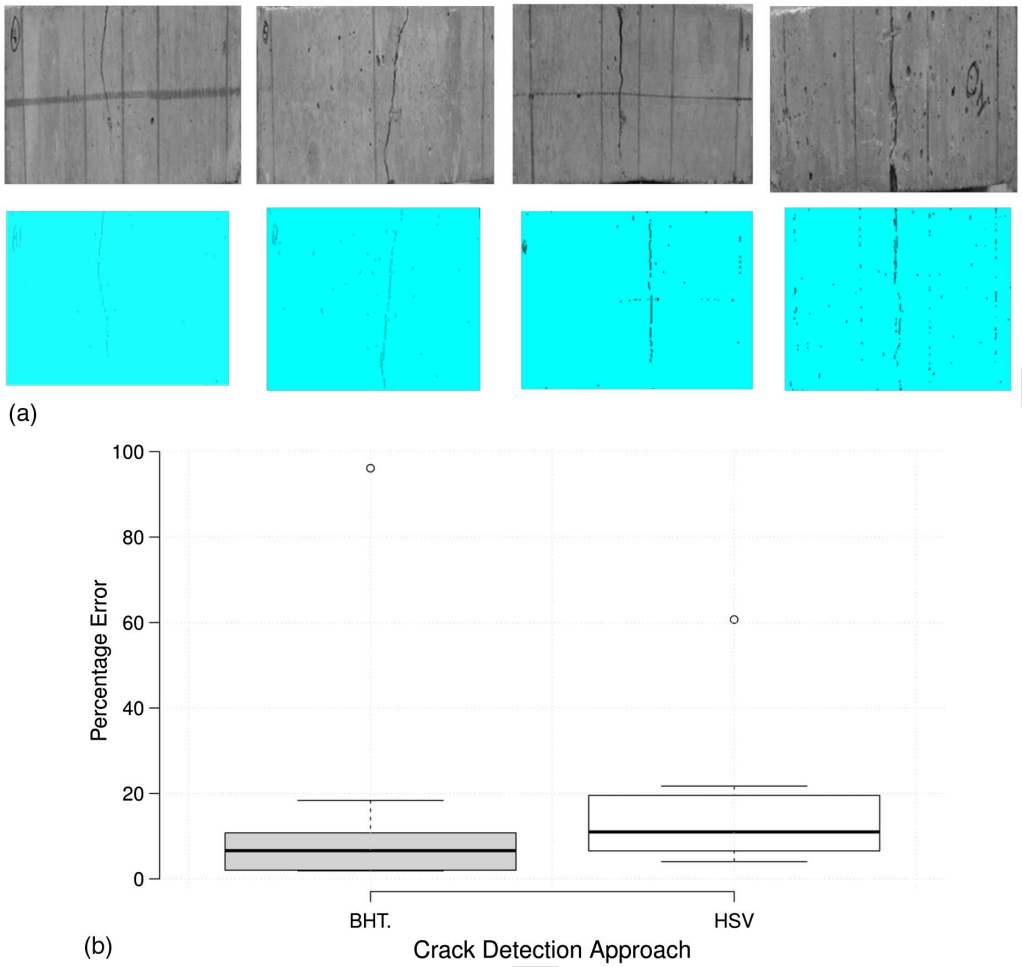

F4:1 **Fig. 4.** (a) Image database of samples with different crack sizes; (b) percentage error for BHT and HSV approach in comparison with actual
F4:2 measurements

represent any cracking. In addition, quantified crack lengths are given in Table 1.

The crack length is obtained by considering all the detected crack pixels (no linearity is assumed). For example, if there are N detected crack pixels (during calibration) where the distance between any pixels corresponds to x cm, then the overall N pixels corresponds to $(N-1)*x$ cm. Therefore, the algorithm performance depends on how effectively filters are performing the classification, and from Fig. 4(a), it is obvious that detection efficiency is acceptable to obtain close to the actual value. The actual measured length of cracks was obtained using a hand-held microscope.

In order to evaluate the overall performance of the developed algorithm, the whisker plots are provided (to show the overall percentage error), as shown in Fig. 4(b). It can be inferred from the plots that BHT and HSV perform with a percentage error of 10 and 20%, respectively. Hence, the structural-based approach is preferable for its exactness and eliminates detection of other surface degradations from cracks.

Table 1. Comparison Table for the Actual Crack Length Versus Algorithm Output

Image	Actual measured length of crack (in cm)	Number of crack pixels	Computed crack length (in cm)
Test image a	10	643	9.18
Test image b	12	872	12.457
Test image c	10.5	793	11.36
Test image d	10	1,022	14.6

Estimation of Surface Quality

The other important aspect of assessing the quality of civil infrastructure is to estimate surface deterioration. Surface degradation is characterized by the formation of color patches or loss of outer layers, resulting in degradation of concrete or masonry surfaces. The primary cause is prolonged exposure to environmental loadings such as heat, moisture, and chemicals. Histogram-based image thresholding has been proven to be an operative strategy to quantify surface deteriorations (Vázquez et al. 2011).

The proposed algorithm requires the user to select the unaffected area in a test image as an initial step. In the subsequent process, thresholding limits are automatically computed to classify the normal and degraded sections. The surface quality of images is assessed through histogram analysis after identifying the affected area from the grayscale of the test images.

The sample images shown in Figs. 5(a and c) are considered for the analysis. The processed images are shown in Figs. 5(b and d). It can be observed that the finishing layer (plaster surface) of the test surface is degraded and severely spalled. To estimate this degradation, the histogram is applied on the test images, and the resulting

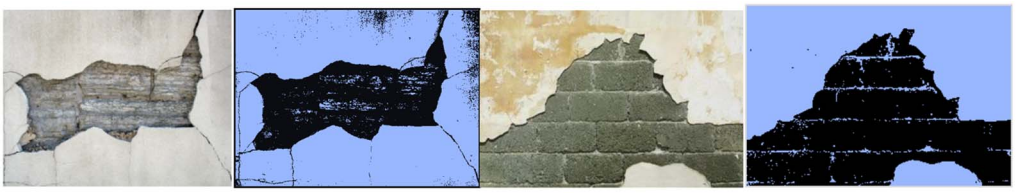

F5:1 **Fig. 5.** Surface quality assessment using the developed image processing tool: (a) test surface 1; (b) test output 1; (c) test surface 2; (d) test output 2

output images are shown in Figs. 5(b and d). The thresholding bounds are extracted from the user-indicated surface area [in Fig. 5(b)] as shown in Fig. 5(a). The damage area is computed in proportion to the image pixels belonging to the affected area.

Development of Graphical User Interface (GUI) and Its Validation

A user-friendly graphical interface has been developed using *MATLAB* functions to examine the structural condition of civil infrastructures. This tool incorporates six structural deteriorations, as shown in Fig. 6, that are considered to be prominent for evaluating the health conditions of structures. For each deterioration, various surface defects are accounted for. For example, for corrosion, there are three different defects that are considered, as shown in Fig. 6, and in which the severity level of damage is rated as minimum (min), moderate (mod), and extensive (ext). The developed image-processing algorithm is integrated into the graphical user interface to quantify the crack and other surface defects. In addition, a fuzzy logic framework to generate MFs is also interfaced with the GUI, where the user can visualize the condition rating of structures. The combination of image processing and fuzzy logic algorithms provides an effective evaluation strategy of civil infrastructures. After selecting the deterioration and corresponding defects, the cumulative damage is assessed as an element condition index. The calculated index value represents the criticality of the structure.

The designed GUI for SHM, as shown in Fig. 6, has two sections wherein fuzzy sets and image algorithms are inculcated. The first section takes into account the deterioration effects based on corrosion, alkali aggregate reaction, fatigue, shrinkage, honeycombing, acid attack, sulfate, and freeze–thaw attack. The other section computes the quantity and quality of the damage based on developed image algorithms. Captured images are loaded into the GUI using the "Load image" option, and, correspondingly, the crack pattern, quantification of crack length, and quality of the surface are computed. The properties of cracks such as thin segmentation and random structural geometry are crucial to determine the length of the crack. Initially, a bottom hat transform filter is adopted to capture thin segmentation, dark nature, and random orientation. The unwanted edges are removed using a Hough-based filter. The standard library tools available in *MATLAB* are used to perform a bottom hat filter, Hough transform, and morphological operations such as erosion and dilation. In the case of detecting surface deterioration, a HSV-based filter technique is implemented. Initially, the algorithm is trained with several images having known crack lengths and, accordingly, thresholding parameters and filter size are optimized. The training algorithm was further used for 20 images having varied crack lengths, and the results were found to be consistent with manual measurements. The processed and original images are further helpful to identify the type of distress that has occurred, and they also can be used to identify global or local damage levels. Image-based distress estimation is further used to quantify the SCI. On the selection of appropriate distress levels and by clicking the "Calculate" button in the GUI, the intensity level of combined distress is automatically computed and the result displayed under "Combined Effect." A sample calculation and the corresponding generation of MF are shown in Fig. 6.

Case Studies

In order to validate the developed tool for civil infrastructures, a southern railway bridge located at Manavur, Tiruvallur, and a storage building located near Avadi, Tamil Nadu, India, were selected as a case study. The discussion presented in this section is limited by a combination of some assumed damage initiation mechanisms and the available list of deterioration codes presented in previous studies.

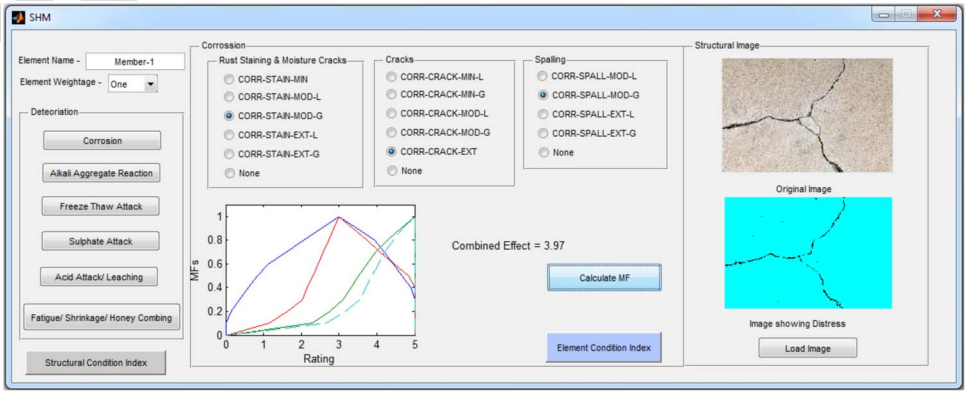

F6:1 **Fig. 6.** SCI evaluation using developed tool; distress and selected MF are for demonstration purposes only

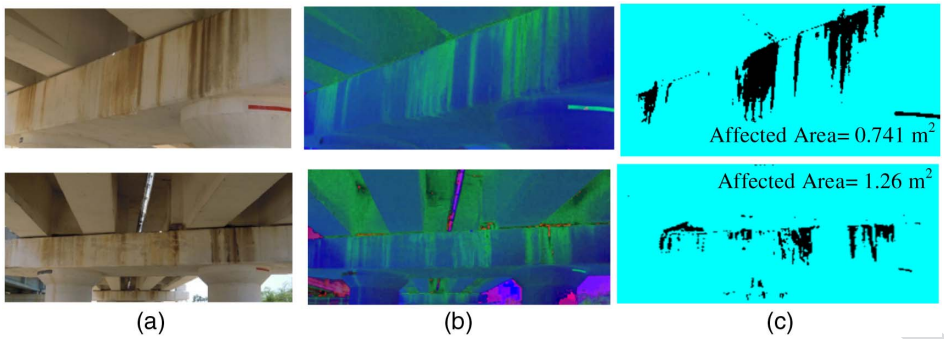

F7:1 **Fig. 7.** Pier cap of railway bridge span 2 and 12: (a) site image; (b) HSV color space; (c) image showing distresses

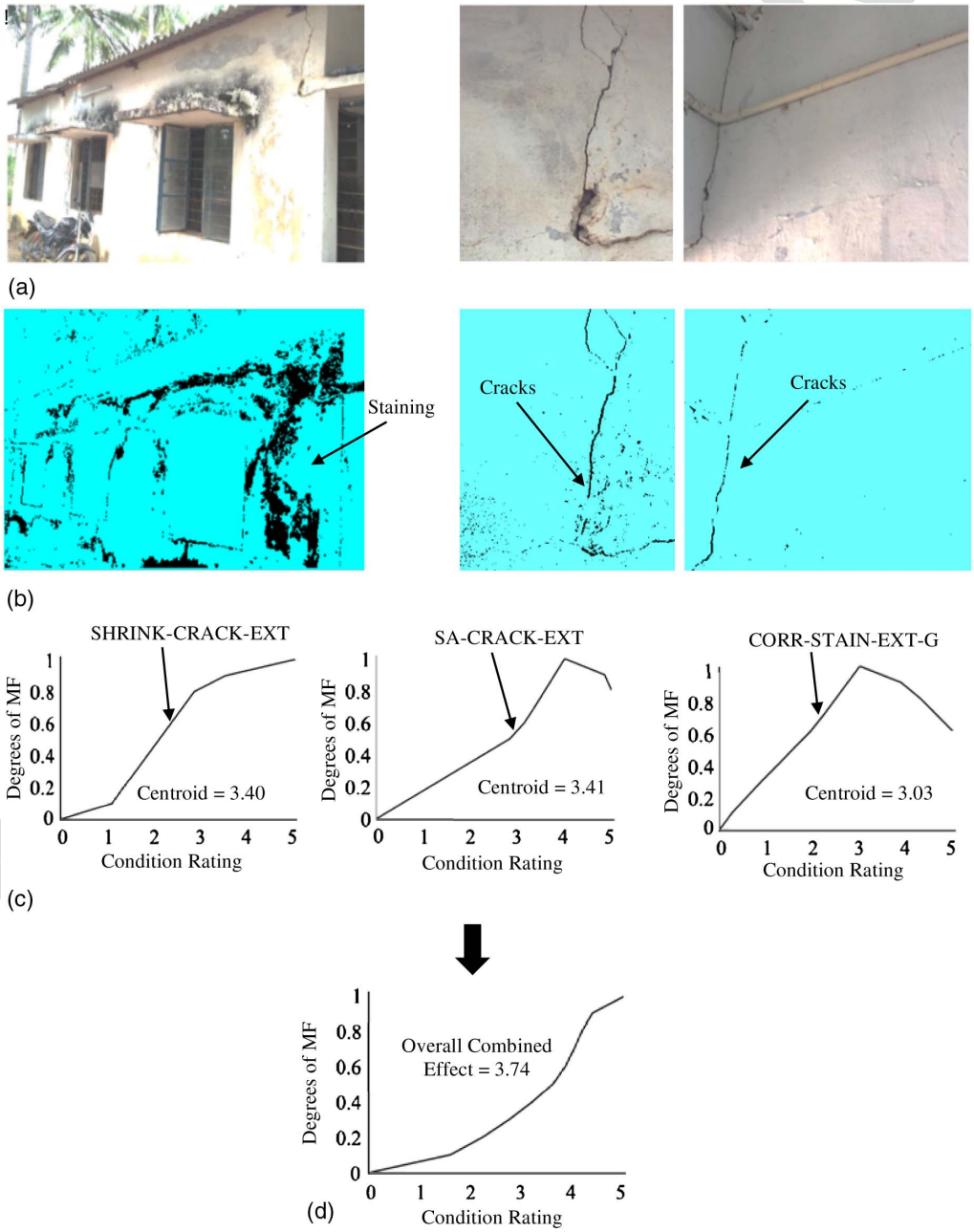

F8:1 **Fig. 8.** East side wall of storage building: (a) unprocessed images; (b) corresponding distress-identified images; (c) effect for each deterioration;
F8:2 (d) overall damage index

Digital images of bridge elements were captured, and it was found that no remarkable damage had occurred on load-bearing elements. However, the authors believe that this bridge has predominantly been affected by heavy rain events and corrosion, which is the primary concern. Sample images shown in Fig. 7(a) were fed into the developed GUI, and the corresponding surface quality was evaluated, as shown in Figs. 7(b and c). At this stage, rather than relying completely on human judgment, the surface staining can be quantified using the image algorithms discussed earlier in this paper, and this value can be very useful in assigning a distress rating level. In Fig. 7(c), it can be observed that the extent of staining seems fairly large; however, because the damage is only superficial (aesthetic only) and not "erosion," the deterioration component under the assigned code is selected as "ACID-ERO-MIN-G." Moreover, because of a lack of a more suitable code in this existing study, "acid attack" has been selected as the primary mechanism. This results in a structural damage condition index of 2.33. Because the bridge does not have any other degradation, the criticality of damage in the bridge structure is deemed minimal.

Similarly, for the condition assessment of the storage structure, a series of photographs are taken. The building is divided into four elements; north side, east side, west side and south side walls.

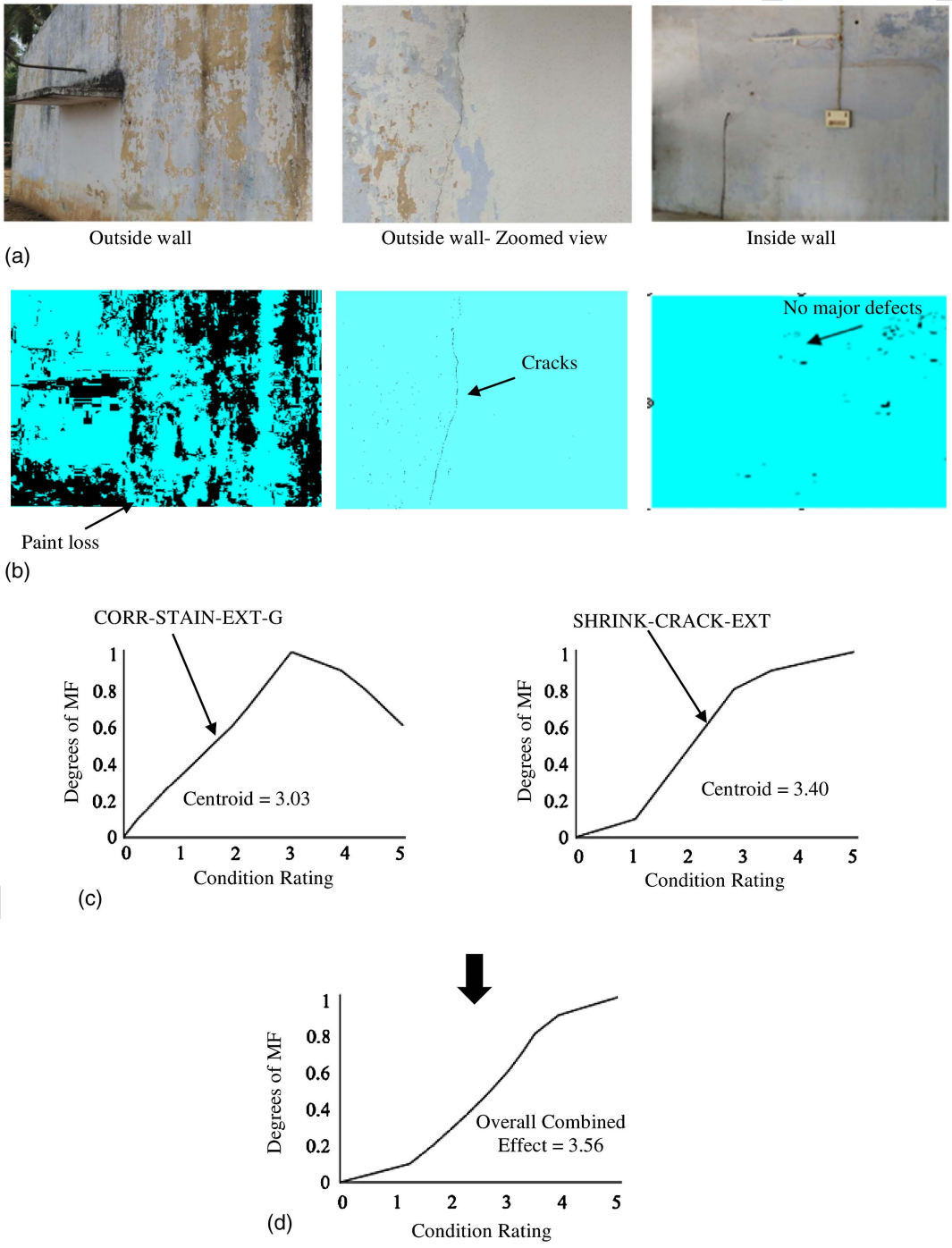

Fig. 9. South side wall of storage building: (a) unprocessed images; (b) corresponding distress-identified images; (c) effect for each deterioration; (d) overall damage index

Fig. 8(a) shows a real image of the outside and inside walls of the selected elements. The north side wall is not considered in this study; it is free from any deterioration because it was covered by asbestos cement roofing sheets. RGB images are fed into the GUI tool to detect the various distresses. Fig. 8 shows the corresponding distress identified for the east wall element based on the developed algorithms. These RGB images and distress-identified images will be used further to select the associated distress codes, which in turn evaluate the condition index for the east side wall element, which is found to be 3.74. Similarly, the condition index is calculated for other walls, as shown in Figs. 9 and 10. SCI considering equal weights for all the elements is calculated as 3.68, as given in Table 2, based on the average weighted method that signifies the criticality of the structure. According to the evaluated SCI, it can be said that the building has the medium damage condition. The entire storage building has been evaluated by considering the condition of each wall (individual MF), and then the overall combined effect of all the walls is considered. As can be seen, the individual wall has a condition rating of approximately 3 and more (because the cracks have a more severe damage condition rating than the surface deterioration), and the combined condition of all the walls turned out to be 3.68.

Conclusion

A GUI tool for rapid estimation of damage indices of civil infrastructure is developed. The formulated protocol uses image functionalities and fuzzy sets to ascertain several structural distresses. Diverse imaging strategies are incorporated to accomplish detection and quantification of structural defects and also to provide a comprehensive evaluation of civil structures. In crack detection,

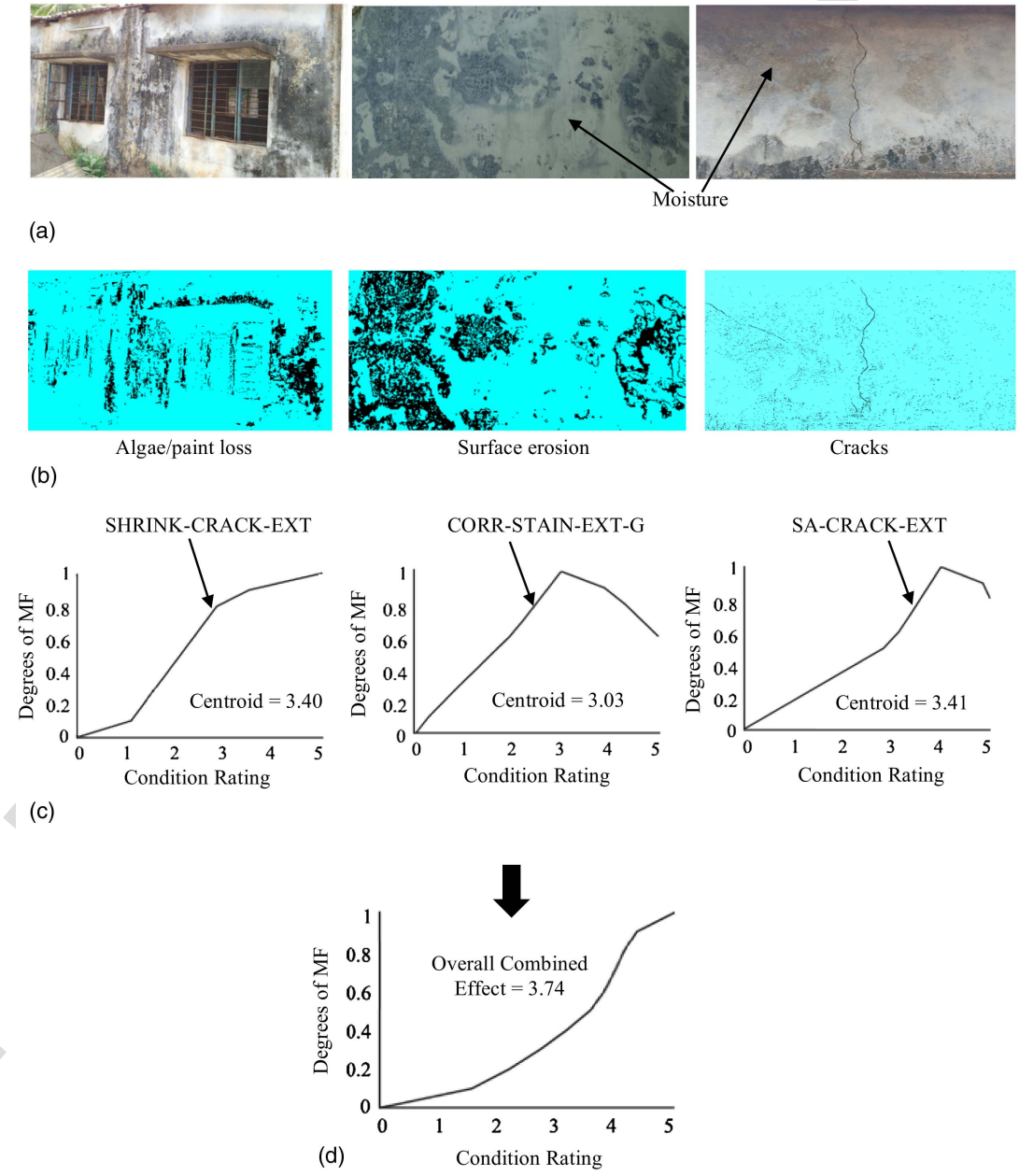

F10:1 F10:2 **Fig. 10.** West side wall of storage building: (a) unprocessed images; (b) corresponding distress-identified images; (c) effects for each deterioration; (d) overall damage index

17 **Table 2.** SCI for the Storage Building

Element name	Element weight	Assigned codes	SCI because of each deterioration mechanism	Combined SCI for each element	Combined SCI for the structure
East wall	1	SHRINK-CRACK-EXT	3.40	3.74	**3.68**
		CORR-STAIN-EXT-G	3.03		
		SA-CRACK-EXT	3.41		
South wall	1	SHRINK-CRACK-EXT	3.40	3.56	
		CORR-STAIN-EXT-G	3.03		
West wall	1	SHRINK-CRACK-EXT	3.40	3.74	
		SA-CRACK-EXT	3.41		
		CORR-STAIN-EXT-G	3.03		

BHT yielded an average error of 5% in comparison with HSV. The surface degradation is effortlessly appraised with the HSV and grayscale thresholding methodologies. A simplified GUI tool is developed in a *MATLAB* environment to ease the assessment of structures. Case studies are presented to examine the level of deterioration. Results reveal that the evaluated bridge attained 2.33 and the storage building 3.68 as the damage index, which signifies the criticality of damage of each structure. In the future, robust sensor modules such as infrared thermal imaging and stereo mapping can be integrated for enhanced data acquisition and structural assessment. This inclusion provides sophisticated hardware-cum-software utility for rapid and effective evaluation of bridges, dams, monuments, buildings, and other structural members.

Appendix. Procedure for the Development of MFs

1. Collect the data from experts or visual inspectors. Table 3 shows the summary of expert responses used in this study;
2. Further tune the data as per the following equations:

$$\text{If } [R_i < R_{i-1} \text{ and } R_i < R_{i+1}],$$
$$\text{then update } [R_i = 0.5(R_{i-1} + R_{i+1})]$$

and

$$\text{If } \left[R_i < 0.1 \times \left(\sum_{i=0}^{5} R_i\right)\right]$$
$$\text{then update } [R_i = 0]$$

3. The obtained numbers are then normalized as

$$\mu_{xi} = \frac{R_i}{\max_{i=0,1,2,\ldots\ldots 5}(R_i)}$$

4. The resulting numbers are shown in Table 4 after tuning; and
5. The obtained MFs are modified using linguistic hedges or modifiers (Mitra et al. 2010) to account for local and global levels of defects, which are given by

$$Local: \mu_{x_i,local} = \mu_{x_i}^{1/2} \quad \text{for } x_i \le x_0$$
$$\mu_{x_i,local} = \mu_{x_i}^{2} \quad \text{for } x_i \ge x_0$$

$$Global: \mu_{x_i,global} = \mu_{x_i}^{2} \quad \text{for } x_i \le x_0$$
$$\mu_{x_i,global} = \mu_{x_i}^{1/2} \quad \text{for } x_i \ge x_0$$

where x_i = condition rating (0–5); and x_0 = condition rating where MF is maximum.

Table 3. Summary of the Expert Responses for Various Distress Conditions (Data from Jain and Bhattacharjee 2012b)

Type of defects because of corrosion	Distress state description	Assigned rating and number of responses					
		0	1	2	3	4	5
Spalling	Depressions less than 20 mm in depth and not exceeding 150 mm in any other dimension	1	5	10	19	10	4
	Depressions of size more than 20 mm in depth with any other dimension greater than 150 mm	0	1	4	9	21	14
Rust staining and moisture marks	Stains visible in isolated patches	10	12	19	8	2	0
	Stains visible covering large area	2	8	11	14	11	5
Cracks	Crack parallel to either stirrups or longitudinal rebars or main rebars, running in one direction only (1D cracks)	1	9	11	16	10	4
	Isolated cracks parallel to both stirrups or longitudinal rebars and main rebars (2D cracks)	0	3	14	15	15	4
	Extensive cracks, spanning in both directions, over relatively large surface area	0	0	4	10	17	20

Note: The following condition rating definitions are considered (based on repair priority). 0: Condition does not require any repair. 1: Very low-priority repair; can be delayed for long span of time. 2: Low-priority repair; actions may be delayed for significant time. 3: Medium-priority repair; actions may be delayed for some time. 4: High-priority repair; urgent actions might be required. 5: Condition is critical; actions must be carried out immediately.

Table 4. Summary of Obtained Condition Indices Based on the Distress State

Type of defects because of corrosion	Distress state description	Condition indices 0	1	2	3	4	5
Spalling	Depressions less than 20 mm in depth and not exceeding 150 mm in any other dimension	0.05	0.26	0.53	1.00	0.53	0.21
	Depressions of size more than 20 mm in depth with any other dimension greater than 150 mm	0.00	0.05	0.19	0.43	1.00	0.67
Rust staining and moisture marks	Stains visible in isolated patches	0.53	0.63	1.00	0.42	0.11	0.00
	Stains visible covering large area	0.14	0.57	0.79	1.00	0.79	0.36
Cracks	Crack parallel to either stirrups or longitudinal rebars or main rebars, running in one direction only (1D cracks)	0.06	0.56	0.69	1.00	0.63	0.25
	Isolated cracks parallel to both stirrups or longitudinal rebars and main rebars (2D cracks)	0.00	0.20	0.93	1.00	1.00	0.27
	Extensive cracks, spanning in both directions, over relatively large surface area	0.00	0.00	0.20	0.50	0.85	1.00

Acknowledgments

The financial assistance extended by Department of Science and Technology, India (DST/INT/Canada/IC—IMPACTS/P-3/2015 (G)) and India-Canada IMPACTS, Centre of Excellence, CANADA under Indo-Canada collaborative project scheme is thankfully acknowledged. We would also like to thank Southern Railways, India, for their onsite technical support.

References

Arliansyah, J., Maruyama, T., and Takahashi, O. (2003). "A development of fuzzy pavement condition assessment." *Japan Soc. Civil Eng.*, 61(746), 275–285.

Blockley, D. I. (1975). "Predicting the likelihood of structural accidents." *Proc. Inst. Civil Eng.*, 59(4), 659–668.

Blockley, D. I. (1977). "Analysis of structural failures." *Proc. Inst. Civil Eng.*, 62(1), 51–74.

Brown, C. B., and Yao, J. T. P. (1983). "Fuzzy sets and structural engineering." *J. Struct. Eng.*, 10.1061/(ASCE)0733-9445(1983)109:5(1211), 1211–1225.

Chang, P., Flatau, C., and Liu, S. C. (2003). "Review paper: Health monitoring of civil infrastructure." *Struct. Health Monitoring*, 2(3), 257–267.

Dong, W., and Shah, H. (1987). "Vertex method for computing functions of fuzzy variables."*Fuzzy Sets Syst.*, 24(1), 65–78.

Dong, Y., Song, R., and Liu, H. (2003). "Bridges structural health monitoring and deterioration detection—Synthesis of knowledge and technology." *Techn. Rep.*, Univ. of Alaska Fairbanks.

Furuta, H., Hirokane, M., Tanaka, S., and Mikumo, Y. (2000). "A study of technology for diagnosing bridge soundness by using portable computer." *Proc. 8th Int. Conf. on Computing in Civil and Building Engineering*, Stanford, CA, 1037–1044.

Fwa, T. F., Liu, S. B., and Teng, K. J. (2003). "Airport pavement condition rating and maintenance-needs assessment using fuzzy logic." *Proc., Airfield Pavements: Challenges and New Technologies*, ASCE, Reston, VA, 29–38.

Hadipriono, F. C. (1988). "Fuzzy set concepts for evaluating performance of constructed facilities." *J. Perform. Constr. Facil.*, 10.1061/(ASCE)0887-3828(1988)2:4(209), 209–225.

Hathout, I. (1993). "Damage assessment of existing transmission towers using fuzzy weighted averages." *Proc., Second Int. Symp. on Uncertainty Modeling and Analysis*, Los Alamitos, CA, 573–580.

Ikhlas, A.-Q., Abudayyeh, O., and Kelly, M. E. (2003). "Analysis of edge-detection techniques for crack identification in bridges." *J. Comp. Civil Eng.*, 10.1061/(ASCE)0887-3801(2003)17:4(255), 255–263.

Jain, K. K., and Bhattacharjee, B. (2012a). "Application of fuzzy concepts to the visual assessment of deteriorating reinforced concrete structures." *J. Const. Eng. Manage.*, 10.1061/(ASCE)CO.1943-7862.0000430, 399–408.

Jain, K. K., and Bhattacharjee, B. (2012b). "Visual inspection and condition assessment of structures [VICAS]: An innovative tool for structural condition assessment." *Int. J. 3R's*, 3(1), 349–357.

Jahanshahi, M. R., Kelly, J. S., Masrim, S. F., and Sukhatme, G. S. (2009). "A survey and evaluation of promising approaches for automatic image-based defect detection of bridge structures." *J. Struct. Infrastruct. Eng.*, 5(6), 455–486.

Jahanshahi, M. R., and Masri, S. F. (2012). "Adaptive vision-based crack detection using 3D scene reconstruction for condition assessment of structures." *Autom. Constr.*, 22, 567–576.

Jahanshahi, M. R., and Masri, S. F. (2013). "A new methodology for non-contact accurate crack width measurement through photogrammetry for automated structural safety evaluation." *Smart Mater. Struct.*, 22(3), 035019.

Kim, Y. M., Kim, C. K., and Hong, S. G. (2006). "Fuzzy based state assessment for reinforced concrete building structures." *Eng. Struct.*, 28(9), 1286–1297.

Lattanzi, D., and Miller, G. R. (2014). "Robust automated concrete damage detection algorithms for field applications." *J. Compt. Civil Eng.*, 28, 2253–2262.

Liang, M. T., Wu, J. H., and Liang, C. H. (2001). "Multiple layer fuzzy evaluation for existing reinforced concrete bridges." *J. Infrastruct. Syst.*, 10.1061/(ASCE)1076-0342(2001)7:4(144), 144–159.

Madau, D. P., and Feldkamp, L. A. (1996). "Influence value defuzzification method". *Fuzzy Syst.*, 3, 1819–1824.

Mamdani, E. H., and Assilian, S. (1975). "An experiment in linguistic synthesis with a fuzzy logic controller." *Int. J. Man Mach. Stud.*, 7(1), 1–13.

Mitra, G., Jain, K. K., and Bhattacharjee, B. (2010). "Condition assessment of corrosion-distressed reinforced concrete buildings using fuzzy logic." *J. Perform Constr. Facil.*, 10.1061/(ASCE)CF.1943-5509.0000137, 562–570.

Nguyen, H.-N., Kam, T.-Y., and Cheng, P-Y. (2012). "A novel automatic concrete surface crack identification using isotropic undecimated wavelet transform." *Intelligent signal processing communication systems*, IEEE, 766–711.

Ogawa, H., Fu, K. S., and Yao, J. T. P. (1984). "An expert system for structure damage assessment." *Pattern Recogn. Lett.*, 2(6), 427–432.

Portland Cement Association. (2002). "Types and causes of concrete deterioration." *IS 536.01*.

Prasanna, P., Dana, K., Gucunski, N., and Basily, B. (2012). "Computer-vision based crack detection and analysis." *SPIE smart structures and materials + nondestructive evaluation and health monitoring*, International Society for Optics and Photonics, 834542.

Rose, P., Aaron, B., Tamir, D. E., Lu, L., and Hu, J. (2014). "Supervised computer-vision based sensing of concrete bridges for crack-detection and assessment." *Transportation Research Board 93rd Annual Meeting*, Vol. 14, Washington DC, 3857.

Ross, T. J. (2005). *Fuzzy logic with engineering applications*, Wiley, Chichester, UK.

Ross, T. J., Sorensen, H. C., Savage, S. J., and Carson, J. M. (1990). "DAPS: Expert system for structural damage assessment." *J. Comput. Civil. Eng.*, 10.1061/(ASCE)0887-3801(1990)4:4(327), 327–348.

Sankarasrinivasan, S., Balasubramanian, E., Karthik, K., Chandrasekar, U., and Gupta, R. (2015). "Health monitoring of civil structures with integrated UAV and image processing system." *11 Int. Conf. on Image & Signal Processing*, Elsevier Procedia Computer Science, Bangalore, India, 508–515.

Sasmal, S., Ramanjaneyulu, K., Gopalakrishnan, S., and Lakshmanan, N. (2006). "Fuzzy logic based condition rating of existing reinforced concrete bridges." *J. Perform Constr. Facil.*, 10.1061/(ASCE)0887-3828(2006)20:3(261), 261–273.

Sasmal, S., and Ramanjaneyulu, K. (2008). "Condition evaluation of existing reinforced concrete bridges using fuzzy based analytic hierarchy approach." *Expert Syst. Appl.*, 35(3), 1430–1443.

Savage, S. J., Ross, T., Sorensen, H., Carson, J., and Satterthwaite, B. (1988). "Development of a rule-based structural damage assessment code." *AFWL-TR-87-19*, Air Force Weapons Laboratory, Albuquerque, NM.

Souflis, C., and Grivas, D. A. (1986). "Fuzzy set approach to linguistic seismic load and damage assessments." *J. Eng. Mech.*, 10.1061/(ASCE)0733-9399(1986)112:6(605), 605–618.

Torok, M., Golparvar-Fard, M., and Kochersberger, K. (2014). "Image-based automated 3D crack detection for post-disaster building assessment." *J. Comp. Civil Eng.*, 10.1061/(ASCE)CP.1943-5487.0000334, A4014004.

Vazquez, M. A., Galan, E., Guerrero, M. A., and Ortiz, P. (2011). "Digital image processing of weathered stone caused by efflorescence: A tool for mapping and evaluation of stone decay." *Constr. Build. Mater.*, 25(4), 1603–1611.

Vidal, M., Ostra, M., Imaz, N., García-Lecina, E., and Ubide, C. (2016). "Analysis of SEM digital images to quantify crack network pattern area in chromium electro deposit." *Surf. Coat. Tech.*, 285, 289–297.

Wang, Y. M., and Elhag, T. M. S. (2007). "A fuzzy group decision making approach for bridge risk assessment." *Comput. Ind. Eng.*, 53(1), 137–148.

Yamaguchi, T., and Hashimoto, S. (2010). "Fast crack detection method for large-size concrete surface images using percolation-based image processing." *Mach. Vision Appl.*, 21(5), 797–809.

Yamaguchi, T., Nakamura, S., Saegusa, R., and Hashimoto, S. (2008). "Image-based crack detection for real concrete surfaces." *IEEE Trans. Electr. Electron. Eng.*, 3(1), 128–135.

Yao, R., and Pakzad, S. N. (2012). "Autoregressive statistical pattern recognition algorithms for damage detection in civil structures." *Mech. Syst. Signal Process.*, 31, 355–368.

Yun, C. B., and Min, J. (2011). "Smart sensing, monitoring, and damage detection for civil infrastructures." *KSCE J. Civil. Eng.*, 15(1), 1–14.

Zhao, J., and Bose, B. K. (2002). "Evaluation of membership functions for fuzzy logic controlled induction motor drive." *28th Annual Conf. on IEE Industrial Electronics Society*, 229–234.

Zou, Q., Cao, Y., Li, Q., Mao, Q., and Wang, S. (2012). "Crack tree: Automatic crack detection from pavement images." *Pattern Recogn. Lett.*, 33(3), 227–238.

Queries

1. Please provide the ASCE Membership Grades for the authors who are members.

2. Please provide the postal code for all the author affiliations.

3. [ASCE Open Access: Authors may choose to publish their papers through ASCE Open Access, making the paper freely available to all readers via the ASCE Library website. ASCE Open Access papers will be published under the Creative Commons-Attribution Only (CC-BY) License. The fee for this service is $1750, and must be paid prior to publication. If you indicate Yes, you will receive a follow-up message with payment instructions. If you indicate No, your paper will be published in the typical subscribed-access section of the Journal.]

4. Please check the hierarchy of section heading levels.

5. Please check all figures, figure citations, and figure captions to ensure they match and are in the correct order.

6. ASCE style for math is to set all mathematical variables in italic font. Please check all math variables throughout the paper, both in equations and throughout the text, to ensure all conform to ASCE style.

7. Duplicate sentence was removed; please confirm the change is acceptable.

8. Please check these ratings for correctness in terms of italics and subscripting throughout.

9. The citation (Jain et al. 2012) mentioned in this sentence is not present in the References list. Please provide the full details and we will insert it in the References list and link it to this citation.

10. ASCE style for fences in math is in the order {[()]}. Please check to ensure all math conforms to this ASCE style.

11. Yamaguchi et al. (2010) has been changed to Yamaguchi and Hasimoto (2010). Please check and confirm.

12. Lattanzi (2014) has been changed to Lattanzi and Miller (2014). Please check and confirm.

13. Equation number “(6)” repeated twice in article, so we have changed it to sequential order. Please check and confirm

14. ASCE style for matrices, vectors, and tensors is to designate them either using bold regular font (e.g., $\mathbf{A}$) or lightface italic font in fences (e.g., $[A]$), but not both. Elements of matrices, components of vectors, and subscripts and superscripts are set in italic. Please check throughout the paper to ensure all matrices, vectors, and tensors conform to this ASCE style.

15. Please confirm change of “red box” to “Fig. 5(b)”. The figures will not print in color.

16. ASCE style requires full reference details for the software "MATLAB”. Please provide the full details for (MATLAB), and we will insert it in the References list and link it to this citation.

17. Please provide significance of "bold" in Table 2.

18. This query was generated by an automatic reference checking system. This reference could not be located in the databases used by the system. While the reference may be correct, we ask that you check it so we can provide as many links to the referenced articles as possible.

19. A check of online databases year found in this reference. Please Add year ’2016’.

20. Please provide the publisher or sponsor name and location (not the conference location) for reference Furuta et al. (2000).

21. Please provide the publisher or sponsor name and location (not the conference location) for reference Hathout (1993).

22. This query was generated by an automatic reference checking system. This reference could not be located in the databases used by the system. While the reference may be correct, we ask that you check it so we can provide as many links to the referenced articles as possible.

23. Please provide issue id for reference Jahanshahi and Masri (2012).

24. This query was generated by an automatic reference checking system. This reference could not be located in the databases used by the system. While the reference may be correct, we ask that you check it so we can provide as many links to the referenced articles as possible.

25. Please provide issue id for reference Lattanzi and Miller (2014).

26. This query was generated by an automatic reference checking system. This reference could not be located in the databases used by the system. While the reference may be correct, we ask that you check it so we can provide as many links to the referenced articles as possible.

27. Please provide issue id for reference Madau and Feldkam (1996).

28. A check of online databases revealed a possible error in this reference. The fpage has been changed from ’13’ to ’1’. Please confirm this is correct.

29. Please provide the publisher or sponsor name and location (not the conference location) for reference Nguyen et al. (2012).

30. Please provide location for reference Portland Cement Association (2002).

31. Please provide location for reference Prasanna et al. (2012).

32. Please provide the publisher or sponsor name and location (not the conference location) for reference Rose et al. (2014).

33. This reference Ross (2005) is not mentioned anywhere in the text. ASCE style requires that entries in the References list must be cited at least once within the paper. Please indicate a place in the text, tables, or figures where we may insert a citation or indicate if the entry should be deleted from the References list.

34. A check of online databases year found in this reference. Please Add year ’2016’.

35. Please provide issue id for reference Vidal et al. (2016).

36. Please provide issue id for reference Yao and Pakzad (2012).

37. This reference Yun and Min (2011) is not mentioned anywhere in the text. ASCE style requires that entries in the References list must be cited at least once within the paper. Please indicate a place in the text, tables, or figures where we may insert a citation or indicate if the entry should be deleted from the References list.

38. Please provide the publisher or sponsor name and location (not the conference location) for reference Zhao and Bose (2002).